



Circular motion of particles suspended in a Gaussian beam with circular polarization validates the spin part of the internal energy flow

Angelsky, O. V. ; Bekshaev, A. Ya. ; Maksimyak, P. P. ; Maksimyak, A. P. ; Mokhun, I. I. ; Hanson, Steen Grüner; Zenkova, C. Yu. ; Tyurin, A. V.

Published in:
Optics Express

Link to article, DOI:
[10.1364/OE.20.011351](https://doi.org/10.1364/OE.20.011351)

Publication date:
2012

Document Version
Publisher's PDF, also known as Version of record

[Link back to DTU Orbit](#)

Citation (APA):
Angelsky, O. V., Bekshaev, A. Y., Maksimyak, P. P., Maksimyak, A. P., Mokhun, I. I., Hanson, S. G., Zenkova, C. Y., & Tyurin, A. V. (2012). Circular motion of particles suspended in a Gaussian beam with circular polarization validates the spin part of the internal energy flow. *Optics Express*, 20(10), 11351-11356. <https://doi.org/10.1364/OE.20.011351>

General rights

Copyright and moral rights for the publications made accessible in the public portal are retained by the authors and/or other copyright owners and it is a condition of accessing publications that users recognise and abide by the legal requirements associated with these rights.

- Users may download and print one copy of any publication from the public portal for the purpose of private study or research.
- You may not further distribute the material or use it for any profit-making activity or commercial gain
- You may freely distribute the URL identifying the publication in the public portal

If you believe that this document breaches copyright please contact us providing details, and we will remove access to the work immediately and investigate your claim.

Circular motion of particles suspended in a Gaussian beam with circular polarization validates the spin part of the internal energy flow

O. V. Angelsky,^{1,*} A. Ya. Bekshaev,² P. P. Maksimyak,¹ A. P. Maksimyak,¹ I. I. Mokhun,¹ S. G. Hanson,³ C. Yu. Zenkova,⁴ and A. V. Tyurin²

¹Correlation Optics Department, Chernivtsi National University, 2, Kotsyubinsky Str., Chernivtsi 58012, Ukraine

²Physical Department, Odessa I.I. Mechnikov National University, Dvorianska 2, Odessa 65082, Ukraine

³DTU Fotonik, Department of Photonics Engineering, DK-4000 Roskilde, Denmark

⁴Department of Optics and Spectroscopy, Chernivtsi National University, 2, Kotsyubinsky Str., Chernivtsi 58012, Ukraine

*angelsky@itf.cv.ua

Abstract: Non-spherical dielectric microparticles were suspended in a water-filled cell and exposed to a coherent Gaussian light beam with controlled state of polarization. When the beam polarization is linear, the particles were trapped at certain off-axial position within the beam cross section. After switching to the right (left) circular polarization, the particles performed spinning motion in agreement with the angular momentum imparted by the field, but they were involved in an orbital rotation around the beam axis as well, which in previous works [Y. Zhao et al, Phys. Rev. Lett. **99**, 073901 (2007)] was treated as evidence for the spin-to orbital angular momentum conversion. Since in our realization the moderate focusing of the beam excluded the possibility for such a conversion, we consider the observed particle behavior as a demonstration of the macroscopic “spin energy flow” predicted by the theory of inhomogeneously polarized paraxial beams [A. Bekshaev et al, J. Opt. **13**, 053001 (2011)].

© 2012 Optical Society of America

OCIS codes: (260.2160) Energy transfer; (260.5430) Polarization; (350.4855) Optical tweezers or optical manipulation; (350.4990) Particles.

References and links

1. L. Allen and M. J. Padgett, “The Poynting vector in Laguerre–Gaussian beams and the interpretation of their angular momentum density,” *Opt. Commun.* **184**(1-4), 67–71 (2000).
2. M. V. Vasnetsov, V. N. Gorshkov, I. G. Marienko, and M. S. Soskin, “Wavefront motion in the vicinity of a phase dislocation: “optical vortex,” *Opt. Spectrosc.* **88**(2), 260–265 (2000).
3. A. Ya. Bekshaev and M. S. Soskin, “Rotational transformations and transverse energy flow in paraxial light beams: linear azimuthons,” *Opt. Lett.* **31**(14), 2199–2201 (2006).
4. A. Ya. Bekshaev and M. S. Soskin, “Transverse energy flows in vectorial fields of paraxial beams with singularities,” *Opt. Commun.* **271**(2), 332–348 (2007).
5. M. V. Berry, “Optical currents,” *J. Opt. A, Pure Appl. Opt.* **11**(9), 094001 (2009).
6. A. Bekshaev, K. Bliokh, and M. Soskin, “Internal flows and energy circulation in light beams,” *J. Opt.* **13**(5), 053001 (2011).
7. K. Y. Bliokh, M. A. Alonso, E. A. Ostrovskaya, and A. Aiello, “Angular momenta and spin-orbit interaction of non-paraxial light in free space,” *Phys. Rev. A* **82**(6), 063825 (2010).
8. M. Born and E. Wolf, *Principles of Optics*, 7th ed. (Pergamon, London, 2005).
9. H. F. Schouten, T. D. Visser, and D. Lenstra, “Optical vortices near sub-wavelength structures,” *J. Opt. B Quantum Semiclassical Opt.* **6**(5), S404–S409 (2004).
10. M. A. Seo, A. J. L. Adam, J. H. Kang, J. W. Lee, S. C. Jeoung, Q. H. Park, P. C. M. Planken, and D. S. Kim, “Fourier-transform terahertz near-field imaging of one-dimensional slit arrays: mapping of electric-field-, magnetic-field-, and Poynting vectors,” *Opt. Express* **15**(19), 11781–11789 (2007).

11. T. Zentgraf, J. Dorfmueller, C. Rockstuhl, C. Etrich, R. Vogelgesang, K. Kern, T. Pertsch, F. Lederer, and H. Giessen, "Amplitude- and phase-resolved optical near fields of split-ring-resonator-based metamaterials," *Opt. Lett.* **33**(8), 848–850 (2008).
12. A. Bitzer, H. Merbold, A. Thoman, T. Feurer, H. Helm, and M. Walther, "Terahertz near-field imaging of electric and magnetic resonances of a planar metamaterial," *Opt. Express* **17**(5), 3826–3834 (2009).
13. N. Fang and X. Zhang, "Imaging properties of a metamaterial superlens," *Appl. Phys. Lett.* **82**(2), 161–163 (2003).
14. M. Ware, W. E. Dibble, S. A. Glasgow, and J. Peatross, "Energy flow in angularly dispersive optical systems," *J. Opt. Soc. Am. B* **18**(6), 839–845 (2001).
15. K. Volke-Sepulveda and R. A. Terborg, "Can diffraction provide quantitative information about energy flux in an optical vortex?" in *Frontiers in Optics, OSA Technical Digest (Optical Society of America, 2011)*, paper JTua38.
16. C.-C. Chen and J. F. Whitaker, "An optically-interrogated microwave-Poynting-vector sensor using cadmium manganese telluride," *Opt. Express* **18**(12), 12239–12248 (2010).
17. R. Khrobatin, I. Mokhun, and J. Viktorovskaya, "Potentiality of experimental analysis for characteristics of the Poynting vector components," *Ukr. J. Phys. Opt.* **9**(3), 182–186 (2008).
18. O. V. Angelsky, M. P. Gorsky, P. P. Maksimyak, A. P. Maksimyak, S. G. Hanson, and C. Y. Zenkova, "Investigation of optical currents in coherent and partially coherent vector fields," *Opt. Express* **19**(2), 660–672 (2011).
19. M. Dienerowitz, M. Mazilu, and K. Dholakia, "Optical manipulation of nanoparticles: a review," *J. Nanophotonics* **2**(1), 021875 (2008).
20. A. Ya. Bekshaev, O. V. Angelsky, S. V. Sviridova, and C. Yu. Zenkova, "Mechanical action of inhomogeneously polarized optical fields and detection of the internal energy flows," *Adv. Opt. Technol.* **2011**, 723901 (2011).
21. A. T. O'Neil, I. MacVicar, L. Allen, and M. J. Padgett, "Intrinsic and extrinsic nature of the orbital angular momentum of a light beam," *Phys. Rev. Lett.* **88**(5), 053601 (2002).
22. V. Garcés-Chavez, D. McGloin, M. D. Summers, A. Fernandez-Nieves, G. C. Spalding, G. Cristobal, and K. Dholakia, "The reconstruction of optical angular momentum after distortion in amplitude, phase and polarization," *J. Opt. A, Pure Appl. Opt.* **6**(5), S235–S238 (2004).
23. Y. Zhao, J. S. Edgar, G. D. M. Jeffries, D. McGloin, and D. T. Chiu, "Spin-to-orbital angular momentum conversion in a strongly focused optical beam," *Phys. Rev. Lett.* **99**(7), 073901 (2007).
24. A. Ya. Bekshaev, "Spin angular momentum of inhomogeneous and transversely limited light beams," *Proc. SPIE* **6254**, 625407, 625407-8 (2006).
25. A. Bekshaev and M. Vasnetsov, "Vortex flow of light: "Spin" and "orbital" flows in a circularly polarized paraxial beam," in *Twisted Photons. Applications of Light with Orbital Angular Momentum* (Weinheim: Wiley-VCH, 2011), 13–24.
26. T. A. Nieminen, A. B. Stilgoe, N. R. Heckenberg, and H. Rubinsztein-Dunlop, "Angular momentum of a strongly focused Gaussian beam," *J. Opt. A, Pure Appl. Opt.* **10**(11), 115005 (2008).
27. A. Ya. Bekshaev, "A simple analytical model of the angular momentum transformation in strongly focused light beams," *Cent. Eur. J. Phys.* **8**(6), 947–960 (2010).
28. O. V. Angelsky, A. Ya. Bekshaev, P. P. Maksimyak, A. P. Maksimyak, S. G. Hanson, and C. Yu. Zenkova, "Orbital rotation without orbital angular momentum: mechanical action of the spin part of the internal energy flow in light beams," *Opt. Express* **20**(4), 3563–3571 (2012).
29. M. E. J. Friese, T. A. Nieminen, N. R. Heckenberg, and H. Rubinsztein-Dunlop, "Optical torque controlled by elliptical polarization," *Opt. Lett.* **23**(1), 1–3 (1998).

1. Introduction

During the past few years, internal energy flows (optical currents) have become a rather appealing and promising topic of physical optics [1–7]. The energy flow pattern, which to some extent and with some limitations is equivalent with the electromagnetic momentum pattern [8], is expressed by the time-averaged Poynting vector distribution and appear as a natural instrument for characterizing light fields with arbitrary structure [5,6]. It is especially suitable in the near-field optics and for description of evanescently decaying waves [9–12], e.g., in plasmonic devices; some novel applications related to micro-resonators, invisibility cloaking, superlensing and metamaterials, essentially employ the controllable Poynting vector fields [11–13]. From a fundamental point of view, optical currents provide a deeper insight into the intimate geometric and dynamic transformation processes that underlie any light field evolution in the course of free or controlled propagation and diffraction [3,6,14,15]. In particular, the macroscopic energy current can be divided into the "orbital" and "spin" contributions which reflect the specific features of internal orbital and spin degrees of freedom of a light field and their particular properties and interrelations [4–7].

However, an essential circumstance complicates the use of internal energy flows as universal light field characteristics: the lack of direct and suitable ways for their detection and/or measurement. In contrast to the multitude of approaches to determine the energy density, the only regular way of determining the energy flow density relies upon measurements of amplitudes and phases of the electric (magnetic) field components [10,16,17] followed by Poynting vector calculation via the definition

$$\mathbf{S} = c^2 \mathbf{p} = gc \operatorname{Re}(\mathbf{E}^* \times \mathbf{H}). \quad (1)$$

Here the field is assumed monochromatic so that the electric and magnetic vectors can be written as $\operatorname{Re}[\mathbf{E} \exp(-i\omega t)]$, $\operatorname{Re}[\mathbf{H} \exp(-i\omega t)]$, ω is the radiation frequency, $g = (8\pi)^{-1}$ in the Gaussian system of units, and c is the velocity of light. In Eq. (1), the connection between the Poynting vector \mathbf{S} and the field momentum density \mathbf{p} is explicitly stated, which permits us, in what follows, to use both quantities \mathbf{S} and \mathbf{p} on equal terms.

This correspondence suggests an alternative way for the energy flow evaluation: since the electromagnetic momentum can be imparted to particles and trigger their motion, the optical currents can be measured by the mechanical action exerted on the probe particles deliberately localized (trapped) within the optical field [18]. Although intuitively evident, this mode of operation is also coupled with substantial difficulties. First of all, the field momentum is not the only reason for the particle motion; together with the electromagnetic ponderomotive influences of non-Poynting origin (gradient force, dissipative force, polarization-dependent dipole force [19,20]), the specific ghost effects may occur due to the medium in which the probe particles are suspended (radiometric, photophoretic forces, the medium viscosity, etc.) and because of the particle shape and material [5,19]. Even in situations where all non-Poynting sources are isolated (e.g., due to special geometry of the field and the measuring equipment [19]), it is rather difficult to establish an exact numerical correspondence between the probe particle motion and the local value of the field momentum: at best, the particles' motion provides only a qualitative picture of the internal energy flows. Nevertheless, this approach appears to be rather suitable in cases where this qualitative picture is sufficient. Among a number of works dealing with the light-induced probe particle motion (for an informative review, see Ref [19].), we mention only a few ones addressed directly at the detection of the probe particle translation, in contrast to the spinning motion, which served to distinguish between the spin and orbital flow actions [21–23].

However, the theory predicts that the spin of the electromagnetic field, naturally associated with its circular polarization, may also produce a macroscopic energy flow that imposes translation of probe particles [5,6,24,25]. At a first glance counter-intuitively, this feature is associated with inhomogeneous distribution of the “fourth” Stokes parameter [8] $s_3(x, y)$ over the cross section of a paraxial beam propagating along the longitudinal axis z ; namely, the transverse spin momentum equals [4,6,25]

$$\mathbf{p}_s = \frac{1}{2\omega c} \left(\mathbf{e}_x \frac{\partial s_3}{\partial y} - \mathbf{e}_y \frac{\partial s_3}{\partial x} \right) = -\frac{1}{2\omega c} [\mathbf{e}_z \times \nabla s_3], \quad (2)$$

where \mathbf{e}_x , \mathbf{e}_y and \mathbf{e}_z are the unit vectors of the coordinate axes, and $\nabla = \mathbf{e}_x (\partial/\partial x) + \mathbf{e}_y (\partial/\partial y)$. In beams with homogeneous circular polarization $s_3(x, y) = \pm I(x, y)$ where $I(x, y)$ is the beam intensity and the upper (lower) sign denotes the right (left) handedness of the field vector rotation. If, additionally, the beam is circularly symmetric and its intensity depends on the transverse radius $r = \sqrt{x^2 + y^2}$ alone, the spin flow (2) is oriented along the circumferences $r = \text{const}$ being numerically equal to [1,25]

$$p_s = \mp \frac{1}{2\omega c} \frac{\partial}{\partial r} I(r). \quad (3)$$

Note that in contrast to the orbital flow that occurs due to the special wavefront morphology (e.g., screw wavefront dislocation associated with the phase vortex structure), the spin flow (2), (3) only depends on the intensity distribution and materialize even in beams with smooth or plane wavefront where the transverse orbital flow vanishes. Recently [6,25] it was suggested that the macroscopic spin flow can be detected via the orbital motion of the probe particles trapped within a circularly polarized beam with inhomogeneous (e.g., Gaussian) intensity distribution. The idea seems rather obvious since it was repeatedly realized for the detection of the orbital circulatory flow [21–23]. However, in applications related to the spin flow it encounters some additional difficulties. The main problem is that the transverse field momentum normally has very low absolute value and, to reach a perceptible level of its action, strong energy concentration in the cell with suspended particles is indispensable, which is achieved by high-NA focusing. But in this case, the initial spin flow of the incident beam is inevitably converted into the orbital flow of the focused beam, associated mainly with its amplified longitudinal component, which acquires a vortex structure [26,27]. As a result, the conversion-generated orbital flow produces essentially similar ponderomotive action, and one cannot definitely distinguish the spin and orbital flow contributions. To circumvent this inconvenience, one should avoid the strong focusing. In fact, this can be accomplished without essential decrease of the spin flow if the field inhomogeneity is properly enhanced: due to Eqs. (1) and (2), deficiency of the beam intensity can be compensated by a growth in $|\nabla I|$. This was recently realized [28] employing the interference between two beams which permitted us to demonstrate the spin flow mechanical action for the first time. In this paper, we present a more direct approach in which, due to the improved radiation source, a moderately focused beam itself contains sufficient spin flow to perform the orbital or (locally) translational motion of the probe particles.

2. Measurements

A sketch of the experimental setup is presented in Fig. 1. The semiconductor laser LD emits linearly polarized radiation with wavelength $\lambda = 650$ nm. The telescopic system TS consists of two positive lenses with a common focal plane, where the pinhole diaphragm (3 mm diameter) is placed. This establishes a collimated near-Gaussian beam of 2.5 mm in diameter. By rotation of the quarter-wave plate QWP (initially the optical axis is orthogonal to the beam polarization plane), we could choose the desired circular or elliptic polarization of the beam. Micro-objective MO with focal distance 12 mm focuses the beam into the quartz cell, which contains the suspended probe particles able to move in the plane orthogonal to the beam axis. The focusing angle is approximately $\alpha = 6^\circ$ (at this condition, in accordance with data of Ref [26], the spin-to-orbital angular momentum conversion does not exceed 1%) and the focal bright spot diameter is close to 3 μ m. The particles' motion is observed with the help of the microscope M and is registered by the digital camera DC.

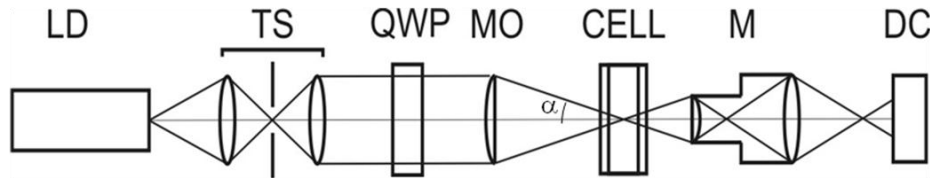


Fig. 1. Schematic of the experimental setup: (LD) semiconductor laser, (TS) telescopic system, (QWP) quarter-wave plate, (MO) micro-objective, (CELL) cell with probing particles suspended in water, (M) microscope, (DC) digital camera.

The beam spot pattern observed in the cell is presented in Fig. 2(b) together with the spin flow maps. The theoretically calculated map shown in Fig. 2(a) is obtained via Eq. (1) from the data of Fig. 2(b). Compared to the theoretical pattern of Fig. 2(a), the really observed spin flow contains irregularities, additional flow loops etc., which are assumed to be due to beam profile instabilities and to the noise factors affecting the registering process. However, the time-average intensity distribution was verified to be close enough to the Gaussian profile, and relative deviation from the Gaussian fitting curve did not exceed 5% at least in the region where the beam intensity is more than 0.3 of maximum.

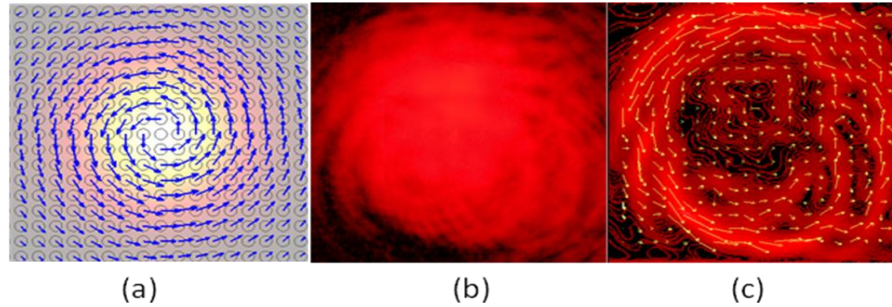


Fig. 2. (a) Theoretical map of the spin flow density \mathbf{p}_s in the focal plane of a circularly polarized Gaussian beam (the transverse intensity distribution with polarization ellipse map is shown as a background, polarization handedness is indicated in the upper right corner); (b) Experimental beam spot pattern in the cell of Fig. 1; (c) The spin flow map for the beam of panel (b) calculated via Eq. (2) (distribution of the spin flow magnitude is shown as a background). In panels (a) and (c) the lengths of the arrows reflect the relative spin flow magnitude.

In the experiment, we used an ensemble of latex micro-particles (refractive index 1.48) suspended in water. The particles were chosen so that their shapes were close to ellipsoids with approximate size $1.5 \times 1 \text{ } \mu\text{m}$, which enabled us to observe the motion of individual particles, including their spinning rotation. The cell position along the longitudinal axis was empirically adjusted so that the trapped particles can be localized several micrometers behind the focal plane. Due to the combined action of the gradient force pulling a particle towards the beam axis, and of the radial light pressure (off-axis energy flow because of the beam divergence), such a procedure permitted the particles to be stably confined at a certain distance from the beam axis [28,29] where the azimuthal spin flow shown in Fig. 2 engages the particles in an orbital rotation. Simultaneously, the particles spin around their centers of mass, which is natural in circularly polarized optical fields [19,29].

As is seen in Fig. 3 and in the attached media, in case of left-polarized beam (1st row of Fig. 3) the particle performs articulate clockwise spinning and orbital motion. Both the orbital and spinning motions stop when the polarization of the incident beam is linear and change their handedness when the beam is right polarized (2nd row of Fig. 3), in full agreement with Eq. (3) and Fig. 2, which confirms the spin nature of the observed motions. However, in the right-polarized case, the counter-clockwise orbital rotation presented in Fig. 3 and [Media 1](#) is not so obvious and could rather be guessed than confidently identified. This can be ascribed to system misalignment when the quarter-wave plate QWP (Fig. 1) was rotated in order to change the polarization handedness, where the focused beam waist might have shifted slightly with respect to the trapped particle position along the z -axis. As a result, the equilibrium between the radial light pressure and the gradient force was destroyed, and the particle occupied a new transverse position near the beam axis where the azimuthal spin momentum is less discernible (see Fig. 2). This interpretation is confirmed by other observations ([Media 2](#)) where the system alignment allowed us to see distinctly the counter-clockwise orbiting in the right-polarized beam, whereas upon switching to opposite polarization the trapped particle was located at the beam axis and visually performed a “pure” spinning rotation.

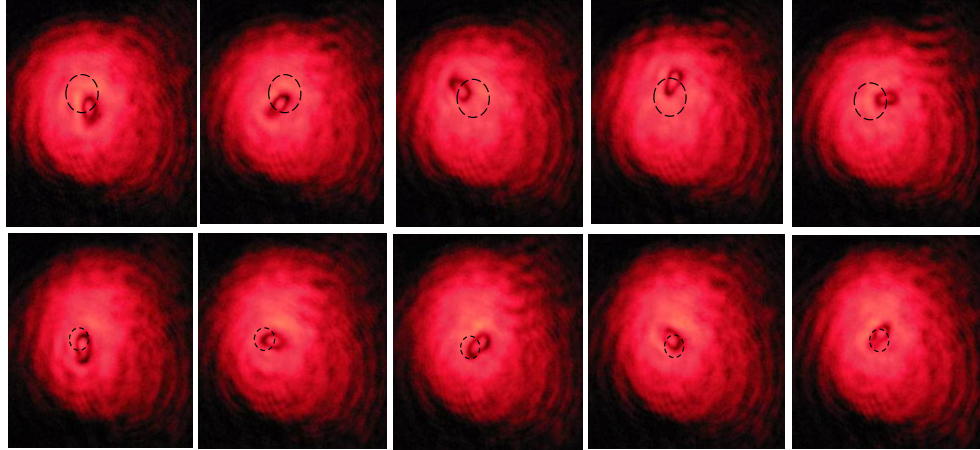


Fig. 3. Consecutive positions of the particle trapped within the beam with (1st row) left, spin + 1, and (2nd row) right, spin -1, circular polarization. Dashed circles show the particle orbits. In 2nd row, the orbital motion is not well accentuated because the particle shifts closer to the beam axis upon switching the polarization, see also [Media 1](#). Similar behavior in other alignment conditions where the particle orbiting is observed in the right-polarized field is demonstrated in [Media 2](#).

3. Conclusions

In summary, the paper illustrates the possibility of controllable motion of suspended particles in moderately focused optical fields with simple spatial structure, where the control is performed by changing the field polarization alone. The presented results confirm the mechanical action of the spin part of the internal energy flow and its ability to cause not only particle spinning but also translational (orbital) motion with transportation of the particle center of mass. This technique will be of importance for optically driven micro-machines and micromanipulation.